

UPDATES ON SCIENTIFIC AND R&D HIGHLIGHTS AT SLAC MeV-UED FACILITY *

F. Ji^{1†}, J. England¹, C. Duncan¹, T. Heinz², P. Kramer¹, R. Lemons¹, F. Liu², Y. Liu¹, M. Mo¹, S. Philip¹, A. Raja³, A. Reid¹, X. Shen¹, S. Weathersby¹, J. Xie⁴, T. Xu¹, A. Zimmerman², Y Zhu⁵

¹SLAC National Accelerator Laboratory, Menlo Park, CA, USA

²Stanford University, Stanford, CA, USA

³Lawrence Berkeley National Laboratory, Berkeley, CA, USA

⁴University of California, Berkeley, CA, USA

⁵Brookhaven National Laboratory, Upton, New York, USA

Abstract

Ultrafast electron diffraction using MeV energy beams (MeV-UED) has enabled unprecedented scientific opportunities in the study of ultrafast structural dynamics in a variety of gas, liquid and solid-state systems. The SLAC MeV-UED program began in 2014 and became an LCLS user facility in 2019. This work will review recent R&D efforts for enhancing the resolution, flux and electron detection of the MeV-UED instrument. Additionally, the integration of AI/ML techniques is being explored to optimize facility operations and accelerate scientific discovery. In all, these will open new avenues for explorations in key areas of ultrafast science.

INTRODUCTION

Ultrafast electron diffraction using MeV energy beams (MeV-UED) has led to a new paradigm in ultrafast electron scattering [1]. MeV electron probes lead to atomic spatial resolution together with sub-picosecond temporal resolution [2]. Furthermore, MeV electrons can provide pure kinetic scattering signals for samples with a given thickness, which makes it possible to achieve quantitative understanding of observables via physics-based modeling. The SLAC MeV-UED program starts in 2014 and became an LCLS-II user facility since 2019. MeV-UED has enabled unprecedented scientific opportunities in ultrafast structural dynamics, including observations of bond dissociation, coherent ground state wavepacket motion after electrocyclic ring-opening, simultaneous observation of electronic and nuclear structure changes in a molecule undergoing non-adiabatic dynamics, hydrogen bond strengthening in liquid water, and phase switches of materials with exotic functional properties. MeV-UED will continue to complement LCLS-II X-ray science and remain the promise of enabling scientific opportunities in key areas. To maximize the science impact of UED, improvements in temporal/spatial resolutions, electron flux and electron detection are required. Figure 1(c) illustrates the current and future performance envelope for the MeV-UED instrument. The solid squares show points on the

current MeV-UED flux/temporal resolution boundary where higher electron flux can be achieved at the expense of temporal resolution. The open squares show the expected performance of MeV-UED following undergoing R&D efforts (upgrade to 1 kHz operation, 1st generation time-tool and laser pump dispersion compensation). Open stars show the performance of a proposed high brightness gun [3] together with an arrival time monitor and hollow-fiber pump laser compression. By pushing the flux/temporal resolution boundary, novel science cases will be enabled. These include resolving structural and electronic dynamics during photo-dissociation events, the study of intramolecular Proton transfer & migration dynamics, investigating momentum-resolved transient phonon populations in thin mono-layer materials, as well as exploring energy pathways and structure-function relationships in hetero-structure based low dimensional systems [4].

In this work, we review recent R&D efforts at the SLAC MeV-UED facility, including the kHz repetition rate upgrade, the adoption of the LCLS ePix10k as a single-electron detector, as well as the integration of AI/ML techniques to optimize operations and accelerate discovery. Collectively, these developments will enhance instrument resolution, increase electron flux, and improve detection efficiency, paving the way for explorations in key areas of ultrafast science.

kHz REPETITION RATE UPGRADE

UED experiment requires high signal-to-noise ratio (SNR) for extraction of weak signals and resolving fs structural dynamics in different systems. Increasing the repetition-rate is the most straightforward way to improve SNR within the same integration time. Practically, choice of repetition rate requires considerations in multiple limiting factors including RF electron source, available laser energy and sample relaxation times. Since 2019, the SLAC MeV-UED facility has routinely operated at 360 Hz for user experiments. Upgrade to 1080 Hz pump-probe data acquisition rate is one of the major effort that has been conducted to further improve the SNR. To this end, both laser and RF systems were improved: an upgrade of the infrared laser system (Ti:Sapphire Coherent Legend Elite Duo + SPA) was completed in April 2021 to accommodate kHz pump&probe experiments. A ScandiNova RF Klystron (Figure 1(d)) has been installed and conditioned

* Work supported by U.S. Department of Energy Office of Science, Basic Energy Sciences under Contract No. DE-AC02-76SF00515, and FWP-10075, 100713, 100940, and 101293

† Corresponding author: fuhaoji@slac.stanford.edu

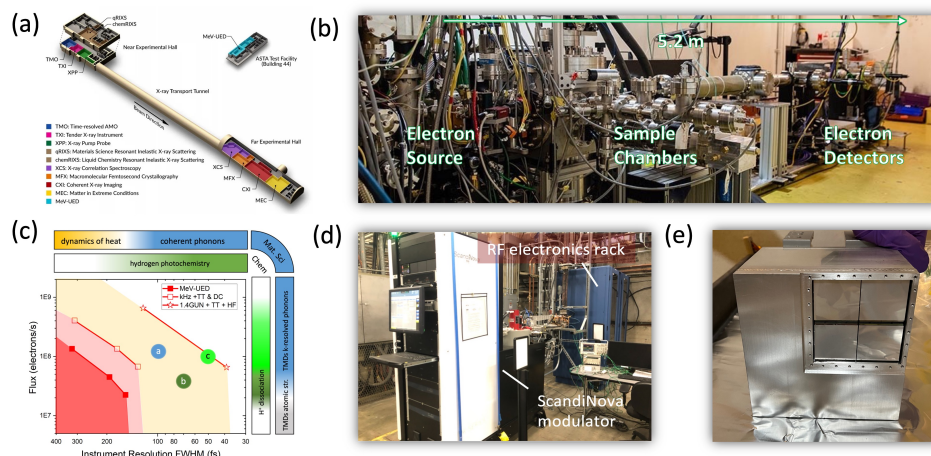


Figure 1: SLAC MeV-UED facility overview and R&D highlights. (a) MeV-UED instrument as part of the LCLS-II user facility. (b) Beam line configuration. (c) the current and future operational envelope for the MeV-UED instrument. (d) The ScandiNova RF Klystron for kHz repetition rate upgrade. (e) ePix10k detector at MeV-UED.

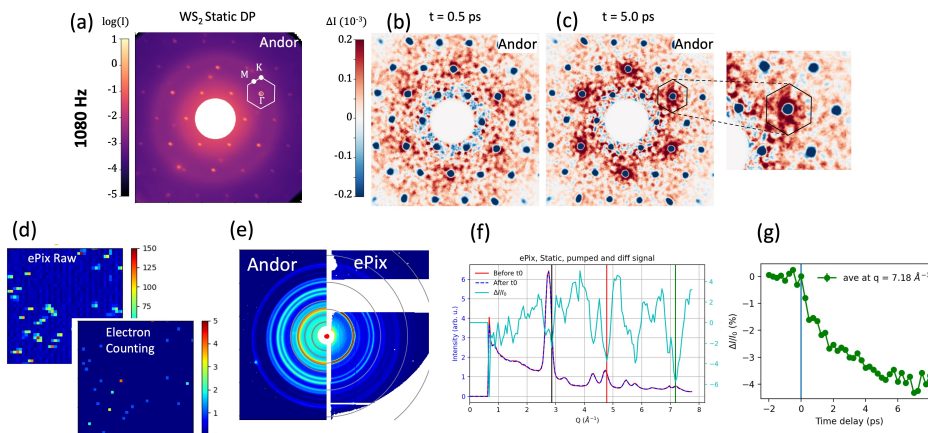


Figure 2: (a) Static MeV-electron diffraction pattern of monolayer MoS₂. (b-c) electron diffuse scattering patterns of MoS₂, data taken at 1080 Hz repetition rate. (d) ePix10k raw data and electron counting results. (e) static diffraction pattern on poly-crystalline Bi. (f,g) pump&probe signals of Bi, data recorded using ePix10k.

to power the S-band (2.856 GHz) high-gradient RF gun at MeV-UED. The Klystron was successfully commissioned in Oct 2024 for 1080 Hz beam operations and UED data acquisition. Figure 2 (a) illustrates the static MeV-electron diffraction pattern of monolayer MoS₂ at room temperature. Electron beam energy was 2.31 MeV and data was collected at 1080 Hz repetition rate. Figure 2 (b) and (c) illustrates the fs electron diffuse scattering patterns on MoS₂ at t = 0.5 and 5.0 ps. Pump laser wavelength was 660 nm and fluence was 14 mJ. As can be clearly seen, the diffuse scattering signals intensities are at 10⁻⁴ level compared to the Bragg peaks, necessitating data acquisition at 1080 Hz to improve the SNR within a practical integration time.

ePix10K AS SINGLE ELECTRON DETECTOR FOR MeV-UED

The existing electron detection system at MeV-UED consists of a P43 phosphor screen coupled to a cooled Andor iXon Electron Multiplying Charge Coupled Device (EM-

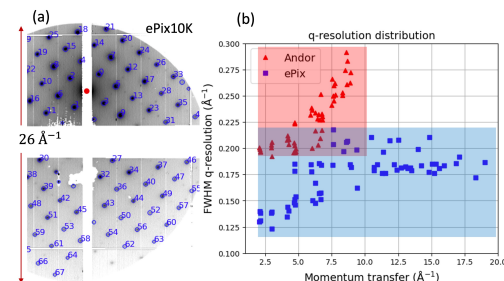


Figure 3: (a) static diffraction pattern from single-crystalline Fe₃O₄ recorded using ePix10k. (b) comparison of FWHM q-resolutions of ePix10k and Andor EMCCD detector at different momentum transfer values.

CCD) camera using a 50 mm f/1.2 telephoto lens. However, this imaging system has several disadvantages. First, the phosphor based detection system is not capable of performing shot-by-shot data collection at 360-1080 Hz, forbidding

shot-by-shot correction of temporal and spatial jitters. Second, the optical imaging system induces significant spherical aberration that can blur the diffraction pattern and reduce q -resolution in the high- q region. Third, in pump&probe experiments, it is crucial to keep scattered pump laser from reaching the detector. This could be done using optical filters but doing so adds the constraint that the pump laser wavelength cannot match the wavelength at which the phosphor fluoresces. It is expected that direct electron detectors would revolutionize the field of MeV-UED, particularly by enabling both spatial and temporal jitter corrections. To this end, the LCLS ePix10k [5] was deployed as a single electron detector at SLAC MeV-UED. Figure 1(e) illustrates the ePix10k detector at MeV-UED. The camera employs a quadrant of the LCLS ePix10k, consisting of four ePix10k modules and 64 analog-to-digital converters (ADCs) with 14 bits pixel depth. The camera is a 0.54 megapixel detector and covers a 8 cm \times 8 cm detection area. Figure 2(d) illustrates a single-shot raw image from ePix10k readout. Single-electron peak finding was conducted based on Landau distribution of electron energy deposition onto the sensor pixels. The electron peak finding algorithm is capable of removing x-ray and detector dark readouts (pedestal) and the resulting image shows a clean electron distribution on the detection area. Figure 2(e) illustrates the poly-crystalline Bismuth static diffraction pattern recorded using Andor EMCCD and ePix10k under same experimental conditions. Figure 2(f) illustrates the radial profile of Bi static diffraction, along with pump&probe difference signal curve obtained using the ePix detector. The two weak diffraction peaks at $q = 6.98 \text{ \AA}^{-1}$ and $q = 7.18 \text{ \AA}^{-1}$ can be clearly resolved due to the improved q -resolution at high q . Figure 2(g) illustrates the pump&probe curve at $q = 7.18 \text{ \AA}^{-1}$, due to improved SNR, a two-stage exponential decay can be clearly seen. Figure 3(a) illustrates the static diffraction pattern from single-crystalline Fe_3O_4 recorded using ePix10k. An end-to-end q range of 26 \AA^{-1} was obtained at 3.12 MeV beam energy. Figure 3(b) shows a direct comparison of the FWHM q -resolution of ePix and Andor EMCCD obtained using Bragg Peak width from Fe_3O_4 pattern. As can be seen, the q -resolution of EMCCD degrades quickly at high q , this is due to the spherical aberration of optical lens system. Meanwhile, the q -resolution of ePix10k remains below 0.22 \AA^{-1} with momentum transfer up to 20 \AA^{-1} , showing clear advantage of ePix10k for resolving tiny and weak features in the high q regions.

AI/ML AND INTELLIGENT SCIENTIFIC FACILITY R&D

Artificial intelligence and machine learning (AI/ML) have recently reached sufficient maturity for applications in real-world tasks. At SLAC MeV-UED, AI/ML techniques has been actively explored to optimize facility operations and accelerate scientific discovery. Recently, the Multi-objective Bayesian Optimization (MOBO) algorithm [6] has been demonstrated at MeV-UED for speeding up online elec-

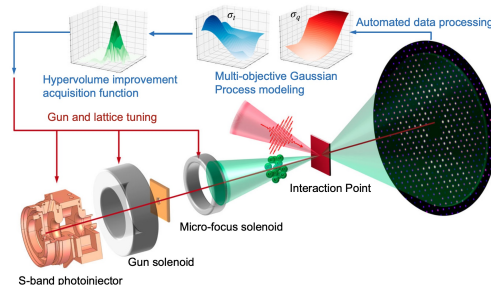


Figure 4: Intelligent scientific facility R&D at SLAC MeV-UED (Reproduced from Ref. [7]). Electron beam properties are extracted from detector readouts and used for constructing GP surrogate models giving overview of machine response in the parameter space. EHVI acquisition function is constructed for efficiently search the parameter space for obtaining PFs.

tron beam tunings and obtaining Pareto Fronts (PFs) giving trade-offs between key beam properties of interest [7]. Such scheme enables an unprecedented overview of the system behavior and takes a significantly smaller number of measurements compared with traditional methods such as a grid scan. Further developments, including two-stage constrained multi-objective Bayesian optimizations (CBE-MOBO) algorithm [8], are being conducted to improve the valid data efficiency and enable PF learning with minimal human inputs. Meanwhile, smart decision-making algorithms in combination with human-in-the-loop methodologies are being developed for facility tuning, fast data analysis and key information extraction (Fig. 4). Ultimately, these will enable intelligent scientific facility operations and maximize scientific outputs at SLAC MeV-UED facility.

CONCLUSION

The SLAC MeV-UED program became an LCLS user facility in 2019 and has enabled unprecedented scientific opportunities in the studies of ultrafast structural dynamics in a variety of gas, liquid and solid-state systems. In this work, we review recent R&D efforts at SLAC MeV-UED, including the kHz repetition rate upgrade, the deployment of the LCLS ePix10k as a single-electron detector and the integration of AI/ML techniques to optimize operations and accelerate discovery. In all, these developments will enhance the instrument resolution, increase electron flux, and improve detection efficiency, enabling new opportunities for explorations in key areas in ultrafast science.

ACKNOWLEDGEMENTS

This work was supported by the U.S. Department of Energy Office of Science, Office of Basic Energy Sciences under Contract No. DE-AC02-76SF00515. M.M. acknowledges the support from the U.S. DOE Office of Science, Laboratory Directed Research and Development program at SLAC under contract DE-AC02-76SF00515, and Fusion Energy Sciences under FWP101242.

REFERENCES

- [1] D. Filippetto *et al.*, “Ultrafast electron diffraction: Visualizing dynamic states of matter”, *Rev. Mod. Phys.*, vol. 94, no. 4, p. 045004, Dec. 2022.
doi:10.1103/revmodphys.94.045004
- [2] SLAC Megaelectronvolt Ultrafast Electron Diffraction Instrument, <https://lcls.slac.stanford.edu/instruments/mev-ued>
- [3] R. J. England *et al.*, “SLAC MeV ultrafast electron diffraction facility upgrade plans”, presented at NAPAC’25, Sacramento, USA, Aug. 2025, paper THP074, this conference.
- [4] Y. Liu, X. Shen, and A. Reid, “UED instrument retreat report”, SLAC National Laboratory, 2023.
- [5] T. B. van Driel *et al.*, “The ePix10k 2-megapixel hard X-ray detector at LCLS”, *J. Synchrotron Radiat.*, vol. 27, no. 3, pp. 608–615, Apr. 2020. doi:10.1107/s1600577520004257
- [6] F. Ji *et al.*, “Multi-Objective Bayesian Optimization at SLAC MeV-UED”, in *Proc. IPAC’22*, Bangkok, Thailand, Jun. 2022, pp. 995–998.
doi:10.18429/JACoW-IPAC2022-TUPOST056
- [7] F. Ji *et al.*, “Multi-objective Bayesian active learning for MeV-ultrafast electron diffraction”, *Nat. Commun.*, vol. 15, no. 1, p. 4726, Jun. 2024. doi:10.1038/s41467-024-48923-9
- [8] F. Ji, *et al.*, “Two-stage constrained Bayesian optimization for particle accelerator tuning”, presented NAPAC’25, Sacramento, USA, Aug. 2025, paper MOP094, this conference.